Kintanar, A., Klevit, R. E., & Reid, B. R. (1987) *Nucleic Acids Res. 14(15)*, 5845-5862.
Kline, A. D., & Wüthrich, K. (1986) *J. Biol. Chem. 192*, 869-890.
Kumar, M. R., Wagner, G., Ernst, R. R., & Wüthrich, K. (1981) *J. Am. Chem. Soc. 103*, 3654-3658.
Lavery, R., & Sklenar, H. (1989) *J. Biomol. Struct. Dyn. 6*, 655-667.
Lefèvre, J.-F., Lane, A. N., & Jardetzky, O. (1987) *Biochemistry 26*, 5076-5090.
Lomonossoff, G. P., Butler, P. J. G., & Klug, A. (1981) *J. Mol. Biol. 149*, 745-760.
Macura, S., & Ernst, R. R. (1980) *Mol. Phys. 1*, 95-117.
Nerdal, W., Hare, D. R., & Reid, B. R. (1988) *J. Mol. Biol.* (in press).
Nigles, M., Clore, G. M., Gronenborn, A. M., Brunger, A. T., Karplus, M., & Nillson, L. (1987a) *Biochemistry 26*, 3718-3733.
Nigles, M., Clore, G. M., Gronenborn, A. M., Piel, N., & McLaughlin, L. W. (1987b) *Biochemistry 26*, 3734-3744.
Noggle, J. H., & Schirmer, R. E. (1971) *The Nuclear Overhauser Effect*, Academic, New York.
Ohlendorf, D. H., & Matthews, B. W. (1983) *Annu. Rev. Biophys. Bioeng. 12*, 259-284.
Otting, G., Widmer, H., Wagner, G., & Wüthrich, K. (1986) *J. Magn. Reson. 66*, 187-193.
Otwinowski, Z., Schevitz, R. W., Zhang, R.-G., Lawson, C. L., Jaudimick, R. O., Marmorstein, B. F., & Sigler, P. B. (1987) *Nature 335*, 321-329.
Rance, M., Sørenson, O. W., Bodenhausen, G., Wagner, G., Ernst, R. R., & Wüthrich, K. (1983) *Biochem. Biophys. Res. Commun. 117*, 479-485.
Redfield, A. G. (1978) *Methods Enzymol. 49*, 253-270.
Rhodes, D. R. (1982) in *Topics in Nucleic Acids Structures* (Neidle, S., Ed.) Part 2, pp 287-304, MacMillen, London.
Scheek, R. M., Russo, N., Boeleus, R., Kaptein, R., & van Boom, J. H. (1983) *J. Am. Chem. Soc. 105*, 2914-2916.
Shakked, Z., Rabinovich, D., Kennard, D., Cruse, W. B. T., Salisbury, S. A., & Viewamitra, A. (1983) *J. Mol. Biol. 166*, 183-201.
States, D. J., Haberkorn, R. A., & Ruben, D. J. (1982) *J. Magn. Reson. 48*, 286-292.
Takeda, Y., Kin, J. G., Caday, C. B., Steers, E., Jr., Ohlendorf, D. H., Anderson, W. F., & Matthews, B. W. (1986) *J. Biol. Chem. 261*, 8608-8616.
Tropp, J., & Redfield, A. G. (1981) *Biochemistry 20*, 2133-2140.
von Hipple, P. H., & McGhee, J. D. (1972) *Annu. Rev. Biochem. 41*, 231-300.
Wagner, G., & Wüthrich, K. (1979) *J. Magn. Reson. 33*, 675-680.
Weber, P. L., Wemmer, D. E., & Reid, B. R. (1985) *Biochemistry 24*, 4553-4562.
Weber, P. L., Brown, S. C., & Mueller, L. (1987) *Biochemistry 26*, 7282-7290.
Wemmer, D. E., Chou, S.-H., & Reid, B. R. (1984a) *J. Mol. Biol. 180*, 41-60.
Wemmer, D. E., Chou, S.-H., Hare, D. R., & Reid, B. R. (1984b) *Biochemistry 23*, 2262-2268.
Williamson, M. P., Havel, T. F., & Wüthrich, K. (1985) *J. Mol. Biol. 182*, 295-315.

Microtubules Accelerate ADP Release by Dynein†

Erika L. F. Holzbaur and Kenneth A. Johnson*
Department of Molecular and Cell Biology, 301 Althouse Laboratory, The Pennsylvania State University, University Park, Pennsylvania 16802

Received November 29, 1988; Revised Manuscript Received April 26, 1989

ABSTRACT: The effects of microtubules on the phosphate–water oxygen exchange reactions catalyzed by dynein were examined in order to determine the mechanism by which microtubules activate the ATPase. Microtubules inhibited the rate of medium exchange observed during net ATP hydrolysis. Inhibition of the exchange reaction was proportional to the extent of microtubule activation of ATP turnover with no effect on the partition coefficient. These data argue that microtubules do not increase the rate of release of phosphate from dynein; rather, they increase the rate of ADP release. Microtubules markedly inhibited medium phosphate–water exchange reactions observed in the presence of ADP and P_i. With increasing concentrations of ADP, the rate of exchange increased in parallel to the dissociation of dynein from the microtubules, suggesting that only free dynein and not the microtubule–dynein complex catalyzes the exchange reaction. The rates of dynein binding to microtubules in the absence and presence of saturating ADP were 1.6×10^6 and 9.8×10^5 M^{-1} s^{-1}, respectively. ADP inhibited the rate of the ATP-induced dissociation of the microtubule–dynein complex with an apparent K_d = 0.37 mM for the binding of ADP to the microtubule–dynein complex. However, the rate of dissociation of ADP from the M·D·ADP complex was quite fast ($\sim$1000 s^{-1}). These data support the postulate of a high-energy dynein–ADP intermediate and indicate that microtubules activate the dynein ATPase by enhancing the rate of ADP release.

Dynein couples the energy of ATP hydrolysis to drive the sliding of adjacent microtubule doublets in the axonemes of eukaryotic cilia and flagella [for reviews, see Gibbons (1981) and Johnson (1985)]. Pre-steady-state kinetic studies have defined the first two steps of the crossbridge cycle for the microtubule–dynein ATPase (Porter & Johnson, 1983b; Johnson, 1983). In Scheme I, which is similar to the Lymn–Taylor scheme for actomyosin (Lymn & Taylor, 1971; Taylor, 1979), the binding of ATP induces the dissociation of the

†This work was supported by NIH Grant GM26726 to K.A.J. K.A.J. was supported by an Established Investigatorship from the American Heart Association with funds contributed in part by the Pennsylvania Affiliate.
*Author to whom correspondence should be addressed.

0006-2960/89/0428-7010$01.50/0

Scheme I

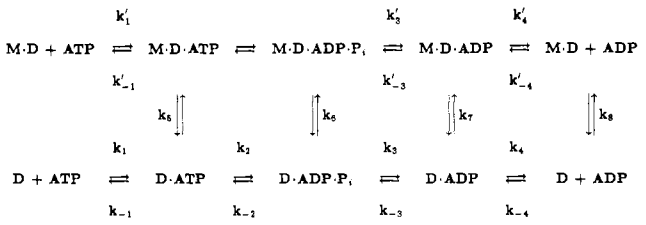

microtubule–dynein complex, and ATP is hydrolyzed on the free dynein head. The observation of a pre-steady-state phosphate burst implies that the rate-limiting step during steady-state turnover is product release. Accordingly, the observation of microtubule activation of steady-state turnover (Omoto & Johnson, 1986) demonstrates that microtubules complete the ATPase cycle by binding to the dynein–products complex.

Phosphate–water oxygen exchange studies have recently identified ADP release, not phosphate release, to be the rate-limiting step during steady-state hydrolysis of ATP by dynein (Holzbaur & Johnson, 1989). In the studies described below, we have analyzed the effects of microtubules on the kinetics of oxygen exchange by dynein in order to investigate the hypothesis that microtubules activate the dynein ATPase by increasing the rate of ADP release.

Materials and Methods

Preparation of Proteins and Nucleotides. Dynein was prepared according to the method of Porter and Johnson (1983a). *Tetrahymena* 22S dynein was purified on sucrose gradients and then dialyzed into 50 mM tris(hydroxymethyl)aminomethane (Tris)[1] and 4 mM $MgCl_2$ for 3 h. Dynein concentrations were determined by the absorbance at 280 nm using an extinction coefficient of 0.97 cm^2/mg (D. Clutter, D. Stimpson, V. Bloomfield, and K. A. Johnson, unpublished results). A molecular weight for dynein of 750000 per site (Johnson, 1983; Shimizu & Johnson, 1983) was used to calculate the molar active-site concentrations for the experiments described.

Tubulin was isolated from the axonemes of *Tetrahymena thermophila* according to the method of Omoto and Johnson (1986). Axonemal tubulin purified in this manner was judged to be pure by analysis of overloaded sodium dodecyl sulfate–polyacrylamide gels. The tubulin was polymerized before each experiment in 100 mM PIPES/4 mM $MgCl_2$, pH 7.0, with 1 mM GTP and 3% dimethyl sulfoxide at 35 °C. These conditions were determined to be optimal for microtubule polymerization, as judged by quantitation of the mass of polymer formed by sedimentation studies and by evaluation of the intact microtubule structure by electron microscopy (Holzbaur et al., 1986). After assembly, microtubules were stabilized by the addition of taxol at a concentration equimolar with tubulin (Schiff et al., 1979; Carlier & Pantaloni, 1983; Porter & Johnson, 1983a). The stabilized microtubules were centrifuged at 178000*g* in Beckman airfuge for 2 min and then resuspended into warm PIPES or Tris buffer.

Tubulin concentrations were determined by the Lowry method with a bovine serum albumin standard. Molar concentrations were calculated by using a molecular weight of 100000 per tubulin dimer (Ponstingl et al., 1981; Krauhs et al., 1981).

[1] Abbreviations: HEPES, *N*-(2-hydroxyethyl)piperazine-*N*′-2-ethanesulfonic acid; MAP(s), microtubule-associated protein(s); PIPES, 1,4-piperazinediethanesulfonic acid; Tris, tris(hydroxymethyl)aminomethane.

ADP was purified by chromatography on DEAE-Sephadex eluted with a gradient of 0.3–0.6 M triethylammonium bicarbonate. Nucleotide purity was verified by thin-layer chromatography on PEI–cellulose developed with 0.85 KH_2PO_4, and by HPLC analysis on a C_{18} column with a mobile phase of 0.1 M K_2HPO_4, 0.025 M tetrabutylammonium hydrogen sulfate, and 18% methanol at pH 7.2.

ATP Regeneration System. In some experiments, the ATP concentration was maintained by a regeneration system of 10 units/mL of pyruvate kinase, 2 mM phosphoenolpyruvate, and 25 mM KCl in 50 mM Tris/4 mM $MgCl_2$ buffer at pH 7.5. The pyruvate kinase concentration was shown to be sufficient to maintain the level of ATP at the highest concentration of dynein used.

ATPase Activity Assays. ATP hydrolysis rates were measured routinely by using the malachite green phosphate assay (Lanzetta et al., 1979) as described (Holzbaur & Johnson, 1986). Alternatively, 7 units/mL lactate dehydrogenase and 0.2 mM NADH were added to the ATP regeneration system, and the disappearance of NADH was monitored as the decrease in absorbance at 340 nm. In some instances, the formation of $[^{32}P]P_i$ from $[\gamma\text{-}^{32}P]ATP$ was measured as described previously (Johnson, 1983).

Phosphate–Water Oxygen Exchange Studies. $P^{18}O_4$ was prepared according to the procedure of Hackney et al. (1980), with an $[^{18}O]$oxygen enrichment of 97%. In order to avoid phosphate contamination, all exchange reactions were performed in acid-washed glassware. Deionized, distilled water was used, and the triethylamine, diazoethane, ethanol, and chloroform were distilled in acid-washed glassware. The exchange reactions were performed at 28 °C in 50 mM Tris/4 mM $MgCl_2$, pH 7.5. The adenylate kinase inhibitor diadenosin pentaphosphate was added at 1 μM to block any possible contaminating activity from the tubulin preparation; although microtubules alone did not catalyze an observable extent of exchange over the reaction time course. Tris buffer was used to avoid interference of anionic buffers (for example, HEPES or PIPES) during isolation of the phosphate.

At each time point, an aliquot was removed from the reaction and vortexed with chloroform to denature the enzyme. Phosphate was isolated from the aqueous phase by ion-exchange chromatography on Bio-Rad AG1-X8 (100–200 mesh, Cl^- form) (Hackney et al., 1980). The purified phosphates were lyophilized and then derivatized with diazoethane. The diazoethane was prepared prior to use from *N*-ethyl-*N*′-nitroso-*N*-nitrosoguanidine from Aldrich Chemical Co. (Domanico et al., 1985). The derivatized phosphates were analyzed by electron-impact gas chromatography–mass spectrometry as described (Holzbaur & Johnson, 1988). The observed $P^{18}O_4$ distributions were compared to theoretical distributions (Hackney, 1980).

In experiments to measure the rate of medium exchange during net ATP hydrolysis, it was necessary to compensate for the production of unlabeled phosphate due to ATP hydrolysis. The net increase in phosphate concentration was measured on aliquots of the reaction mixture over the time course. The isotopic distributions were then corrected for this increase in $P^{16}O_4$ with time due to the hydrolysis of ATP. The fitting program iteratively approached a best fit to the observed distributions of the labeled phosphates while allowing the relative concentration of unlabeled phosphate to vary. This method allows the separation of the two pathways for the accumulation of $P^{16}O_4$ arising from the exchange of water oxygens into the labeled phosphate, and from the hydrolysis of unlabeled ATP. The calculated distributions gave a good

fit to the exchange data and to the measured rate of ATP hydrolysis by the dynein.

Gel Electrophoresis. Sodium dodecyl sulfate–polyacrylamide gel electrophoresis was performed according to the procedure of Laemmli (1970) with the modifications of Porter and Johnson (1983a). Gradient gels of 5–15% acrylamide were run and then stained with the Coomassie blue dyes of Fairbanks et al. (1971). The stained gels were scanned with an LKB 2202 Ultrascan laser densitometer in order to quantitate the relative amounts of dynein per lane.

Stopped-Flow. Kinetics of the dissociation and formation of the microtubule–dynein complex were monitored by stopped-flow as described (Porter & Johnson, 1983b). Light scattering was measured at 420 nm perpendicular to the incident beam, or in some experiments as the absorbance at 420 nm. All stopped-flow experiments were performed in a buffer of 50 mM PIPES/4 mM $MgCl_2$, pH 7.0 at 28 °C. The tubules were sonicated 3 times for 1 s to reduce the average length of the microtubules (Porter & Johnson, 1983b). The use of axonemal tubulin resulted in some increase in the flow birefringence artifact over that observed with tubules polymerized with protein isolated from bovine brains (Porter & Johnson, 1983b; Omoto & Johnson, 1986). However, the resulting traces could be fit sufficiently well by disregarding the artifacts in the early times of the traces.

Data Fitting. Stopped-flow time courses were fit to a single exponential as described (Porter & Johnson, 1983; Johnson, 1986), or by simulation using the KINSIM program (Barshop et al., 1983). The ADP concentration dependence of the dissociation of dynein from the microtubule and the rate of medium exchange (Figure 2) were fit to the equation:

$$\theta = \frac{K^3[\mathrm{ADP}]^3}{1 + K[\mathrm{ADP}] + K^2[\mathrm{ADP}]^2 + K^3[\mathrm{ADP}]^3}$$

where K is the apparent binding constant for ADP and θ is the fraction of dynein molecules with three sites occupied by ADP. Inhibition of the rate of ATP-induced dissociation by the binding of ADP to the microtubule–dynein complex was fit to the equation: $k_{obs} = k_1[\mathrm{ADP}]/(1 + K[\mathrm{ADP}])$. In each case, the data were fit to the equation by nonlinear regression.

Results

Effect of Microtubules on Medium Exchange during Net ATP Hydrolysis. Our previous work demonstrated that dynein catalyzes medium phosphate–water oxygen exchange during net ATP hydrolysis, implying that ADP release was rate limiting during the steady state (Holzbaur & Johnson, 1988). To explore the mechanism by which microtubules activate the steady-state ATP turnover, we first examined the effect of microtubules on the medium exchange reaction during net ATP hydrolysis.

Microtubules activate the dynein ATPase under two conditions (Omoto & Johnson, 1986). At saturating ATP concentration, a high concentration of microtubules is required to activate turnover in a reaction which is limited by the rate of binding of the dynein–products complex to the microtubules. At low ATP concentration, activation is less dependent upon microtubule concentration and is attributable to the reactions of individual heads of a dynein molecule transiently tethered to the microtubules. Because each effect of the microtubules should alter the rate-limiting step of the pathway, we examined medium exchange under each condition.

The time courses of loss of the fully labeled phosphate species during ATP turnover at 4 μM ATP in the presence and absence of microtubules (7 μM polymerized tubulin) are

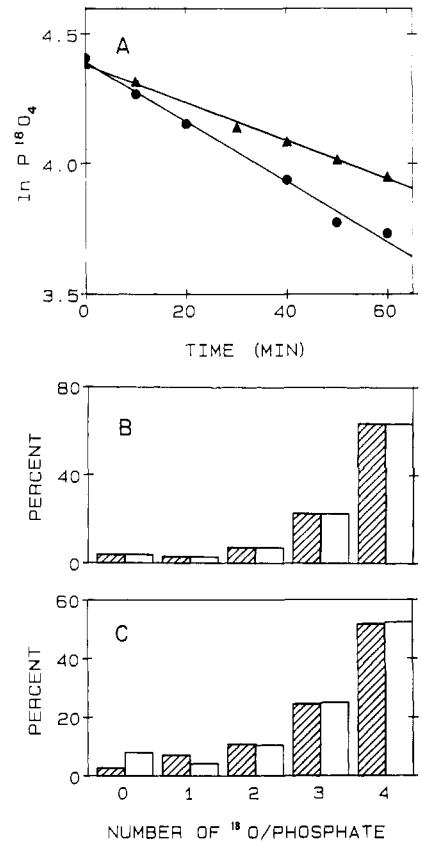

FIGURE 1: Effect of microtubules on medium exchange during net ATP hydrolysis. (A) The time course of washout of ^{18}O from $P^{18}O_4$ (1 mM) catalyzed by dynein (0.1 μM) is shown in the absence (●) and in the presence (▲) of 0.7 mg/mL microtubules during the hydrolysis of 4 μM ATP. The ATP concentration was maintained by using the pyruvate kinase–phosphoenolpyruvate regeneration system in 50 mM Tris/4 mM $MgCl_2$, pH 7.5, buffer at 28 °C. The observed isotopic distributions were corrected for the dilution of the phosphate pool due to the hydrolysis of unlabeled ATP. The curve shows the logarithm of the percent $P^{18}O_4$ versus time of incubation. (B) The corrected exchange pattern for dynein (hatched bars) is compared to the theoretical distribution calculated from the best-fit partition coefficient of 0.30 (white bars). (C) The corrected exchange pattern for the microtubule–dynein complex (hatched bars) is compared to the theoretical distribution calculated from the best-fit partition coefficient of 0.32 (white bars).

shown in Figure 1A. Microtubules activated the dynein ATPase by 2.2-fold under these conditions (data not shown), while the apparent rate of phosphate binding, as measured by the rate of loss of $P^{18}O_4$, was inhibited 1.7-fold.

The best fits to the partition coefficients are compared to the observed distributions in Figure 1B,C. Exchange by dynein was adequately fit to a single partition coefficient of 0.30 in the presence or absence of microtubules.

The measurement of medium exchange during net ATP hydrolysis was repeated several times at both 1 and 5 mM $P^{18}O_4$, and at varying concentrations of microtubules. In all cases, activation of the dynein steady-state ATPase by microtubules was accompanied by a proportional inhibition of the rate of exchange, while no significant alteration in the partition coefficient was noted.

Microtubule activation of the dynein ATPase at saturating ATP (1 mM) was examined in the absence and presence of 18.7 mg/mL tubulin (187 μM tubulin dimers). Under these conditions, microtubules enhanced the rate of ATP turnover 1.4-fold and inhibited the rate of loss of the fully labeled phosphate species by 1.2-fold (data not shown). Microtubules had no effect on the partition coefficient of 0.3, in agreement with the results obtained at low ATP concentration (Figure

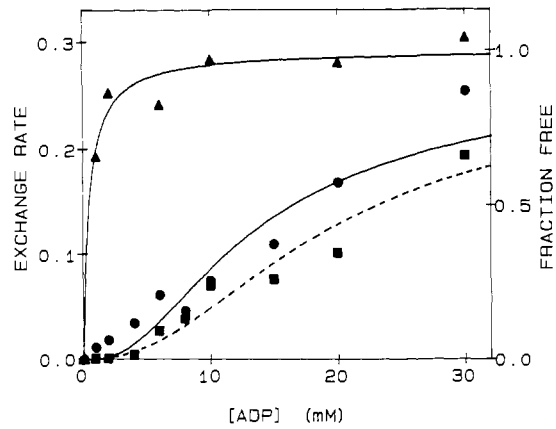

FIGURE 2: ADP concentration dependence of the rate of medium exchange. The rate of loss of $P^{18}O_4$ as a function of the ADP concentration for the medium exchange reaction catalyzed by 0.1 μM dynein in the absence (▲) and presence (●) of 6 μM tubulin. The samples were incubated with 20 mM $P^{18}O_4$ in 50 mM Tris and 4 mM $MgCl_2$, pH 7.5 at 28 °C. The rates of loss of $P^{18}O_4$ are given in units of $s^{-1} \times 10^3$. The curve for exchange by free dynein is hyperbolic with an apparent K_d = 0.48 mM. The curve for the exchange by dynein in the presence of microtubules is modeled as a function of the complete dissociation of dynein assuming three identical independent nucleotide binding sites with an apparent K_d = 10 mM. The fraction of dynein released from microtubules was determined by the cosedimentation assay quantitated by densitometry of Coomassie blue stained gels (■). The dashed curve (- - -) was calculated as the best fit to an equation giving the fraction of dissociated molecules assuming three identical and independent heads, each with an apparent K_d of 13 mM.

1). Although the activation is somewhat lower than is expected (Omoto & Johnson, 1986), possibly due to the high phosphate concentration, the results support the conclusion that microtubules do not alter the rate of phosphate release. Rather, the increase in steady-state turnover rate parallels the decrease in the apparent concentration of dynein–ADP as measured by the rate of loss of the $P^{18}O_4$ label.

Medium Exchange by the Microtubule–Dynein Complex. The effect of microtubules on medium exchange in the presence of ADP was examined next. An initial experiment showed that at ADP concentrations of up to 10 mM, microtubules had a large inhibitory effect on the rate of exchange. These data suggested either that ADP (at millimolar concentrations) does not bind to the microtubule–dynein complex or that phosphate is unable to bind to the M·D·ADP complex in reactions to drive the synthesis of ATP.

To further explore the basis for the inhibition of exchange by microtubules, the ADP concentration dependence of the observed rates of loss of the fully labeled phosphate species was measured in the presence and absence of microtubules (Figure 2). The exchange reactions were fit to a partition coefficient of 0.3 in the presence or absence of microtubules (data not shown), again arguing that the microtubules did not affect the rate of phosphate release.

The ADP concentration dependence of the rate of exchange fit a hyperbola in the absence of microtubules, defining a K_d = 0.48 mM for ADP binding as described previously (Holzbaur & Johnson, 1989). In contrast, the concentration dependence in the presence of microtubules was sigmoidal, suggestive of a multiple binding reaction. These data could be fit to a third-order equation indicative of three independent sites with an apparent K_d = 10 mM, under the assumption that only the free dynein catalyzed the exchange reaction (see Materials and Methods).

To test the postulate that only free dynein catalyzed the exchange reaction, samples were taken during the time course of the exchange reaction and analyzed to determine the fraction of dynein bound to microtubules. After 40 min of reaction, an aliquot of each reaction mixture was removed and was centrifuged to remove dynein bound to microtubules. Samples were analyzed by densitometry of Coomassie blue stained gels to quantitate the amount of dynein in the supernatant. The results shown in Figure 2 demonstrate that dynein was released from the microtubules as the ADP concentration of the reaction increased (■). Moreover, the increase in the rate of exchange parallels the increase in concentration of free dynein molecules in the reaction mixture. These data suggest that the microtubule–dynein complex does not catalyze the exchange reaction. Rather, the high concentrations of ADP drive the dissociation of the dynein from the microtubule in the presence of phosphate, and the free dynein–ADP–P complex catalyzes the exchange reactions.

It is possible that the dissociation of dynein from the microtubules observed in the above experiment occurred due to the increasing ionic strength of the reaction solutions. To test this, microtubule–dynein binding was investigated as a function of ionic strength. At potassium acetate concentrations of up to 200 mM, the dynein did not dissociate from the microtubules (data not shown).

Inhibition of the ATP-Induced Dissociation of the Microtubule–Dynein Complex by ADP. In order to estimate the binding constant of ADP for the microtubule–dynein complex, and to measure the rate of dissociation of the ADP from the M·D·ADP ternary complex, we examined the effect of ADP in inhibiting the rate of ATP-induced dissociation of the microtubule–dynein complex. The microtubule–dynein complex was preincubated with varying concentrations of ADP from 0 to 4 mM and then mixed in the stopped-flow with ATP at a concentration of 50 μM. The ATP-induced dissociation of dynein from the microtubule followed a single exponential at every concentration examined (data not shown).

We initially expected the dissociation kinetics to be biphasic, with a rapid ATP-induced dissociation of any free M·D, followed by a slower rate dependent upon the rate at which ADP dissociated from the M·D·ADP complex. If the dissociation of ADP from the M·D·ADP complex were rate limiting, the time course for ATP-induced dissociation would have been biphasic at concentrations of ADP comparable to the apparent K_d. However, the observed kinetics could be fit to a single exponential at all concentrations of ATP and ADP examined, and the full amplitude of the dissociation reaction was always seen at a rate slower than expected for ATP-induced dissociation of M·D.

The ADP concentration dependence of the rate of dissociation at a fixed ATP concentration is shown in Figure 3A. The data could be fit to a hyperbola with a half-maximal rate at 0.37 mM ADP and a rate asymptotically approaching zero at infinite ADP concentration.

If the dissociation of ADP from M·D·ADP is fast such that the M·D·ADP $\rightleftarrows$ M·D + ADP reaction is assumed to be at equilibrium, then the observed rate of dissociation will be equal to the rate of ATP binding multiplied by the fraction of dynein sites without ADP bound. Substitution from the equilibrium expression yields the equation: $k_{obs} = k_1[ADP]/(1 + K[ADP])$. Thus, a plot of the observed rates of dissociation as a function of the ADP concentration should yield a hyperbola with a half-maximal rate at the K_d for ADP binding to M·D. The data suggest that ADP binds in a rapid equilibrium with an apparent K_d = 0.37 mM.

It can be seen that the fit deviates somewhat from the data at the higher concentrations of ADP. At 4 mM ADP, the fit

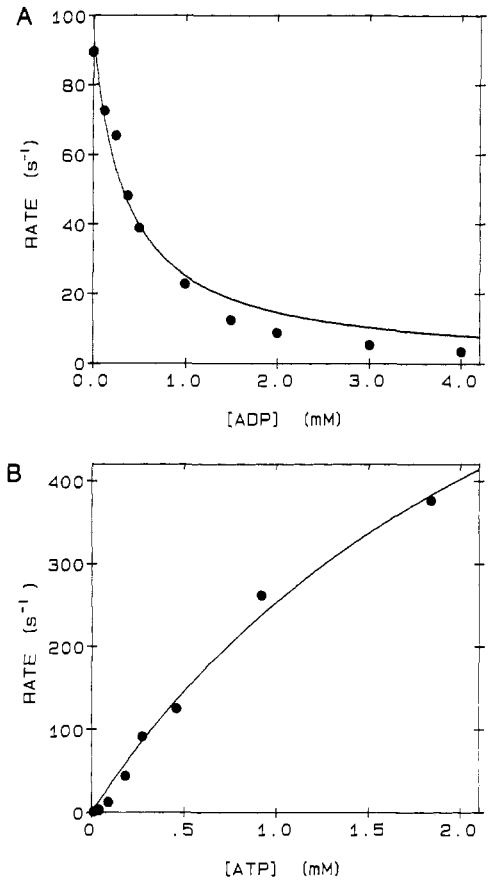

FIGURE 3: Inhibition by ADP of the ATP-induced dissociation of the M·D complex. The rate of ATP-induced dissociation of the microtubule–dynein complex (0.1 mg/mL tubulin, 0.25 mg/mL dynein) was determined by stopped-flow light-scattering measurements. In each case, the data could be accurately fit to a single exponential to estimate the rate. (A) ADP concentration dependence at fixed [ATP]. The microtubule–dynein complex was incubated with varying concentrations of ADP and then mixed with 50 μM ATP with the stopped-flow. The concentration dependence of the rate of dissociation was fit to a hyperbola with a half-maximal rate at 0.37 mM ADP (smooth line) with the rate asymptotically approaching zero. (B) ATP concentration dependence at fixed [ADP]. The microtubule–dynein complex was mixed with varying concentrations of ATP in the presence of 4 mM ADP. The line represents the best fit to a hyperbola with a maximum rate of 970 s^{-1} and a half-maximal rate at 2.8 mM ATP.

predicts a rate which is twice the observed rate. This can be understood in terms of the multiple heads of the dynein. The KINSIM program (Barshop et al., 1983) was used to model the reaction both for a single-site model and for a three-headed model, and the light-scattering signal was interpreted as being due to the dissociation of each head (Holzbaur and Johnson, unpublished results). However, if dynein is bound to the microtubule by three heads, when a single head binds ATP and dissociates it has a finite chance of hydrolyzing the ATP and rebinding to the microtubule before the dissociation of the whole molecule. Inclusion of the rebinding step in the model results in a slower apparent rate of dissociation and accounts for the deviation of the data from the fit in Figure 3A.

We also examined the ATP concentration dependence of the rate of dissociation at a fixed ADP concentration. A concentration of 4 mM ADP was chosen as sufficient to saturate the M·D complex with ADP. The data (Figure 3B) could be fit to a hyperbola extrapolating to a maximum rate of $\sim$1000 s^{-1} at saturating ATP, with a half-maximal rate at 2.8 mM. These data demonstrate that the rate of dissociation of ADP from the M·D·ADP complex, which limits the rate of the reaction at saturating ATP concentration, must be $\sim$1000 s^{-1}. This is an important observation indicating that ADP release from this M·D·ADP complex does not limit the rate of the maximum microtubule-activated ATPase.

Effect of ADP on the Rate of Dynein Binding to Microtubules. The rate of binding of dynein to microtubules was determined in the absence and presence of ADP. The dynein concentration was maintained at a ratio of 0.3 mg of dynein to 1 mg of tubulin, giving a 10-fold molar excess of tubulin sites, as described by Omoto and Johnson (1986). The resulting traces gave satisfactory fits to a single exponential (data not shown). The dependence of the rate of association on the concentration of tubulin defines the second-order rate constant for dynein binding to the microtubule. Values of 1.6×10^6 and 9.8×10^5 M^{-1} s^{-1} were observed in the absence and presence of 4 mM ADP, respectively. Thus, only a small effect of ADP was observed on the rate of dynein binding to microtubules.

Discussion

We examined the effects of microtubules on the kinetics of medium exchange during net ATP hydrolysis catalyzed by dynein at a low ATP concentration. Microtubules inhibited the rate of exchange in proportion to their effect in stimulating the rate of steady-state turnover. Under the conditions of the experiment, dynein is only partially dissociated from the microtubules during the steady state such that the observed activation is due to the tethering of dynein to the microtubules via one or more of its heads (Omoto & Johnson, 1986). The rate of loss of $P^{18}O_4$ is a function of the rate of phosphate binding and the concentration of the D·ADP intermediate. The data suggest that the rebinding of the D·ADP complex to the microtubule leads to a decreased population of the D·ADP by accelerating the rate of ADP release without affecting the rate of phosphate release.

It is interesting to note that the other microtubule motor, kinesin, has an ATPase pathway more like dynein than myosin. Recent studies by Hackney (1988) demonstrated that microtubules accelerate the rate of ADP release by kinesin, which is rate limiting in the steady state.

Studies on the actomyosin ATPase have shown that the rebinding of the myosin–products complex to the actin stimulates the rate of phosphate release and with a corresponding change in the partition coefficient (Hackney & Clark, 1984). In the current work, the partition coefficient for phosphate–water oxygen exchange was not altered by the microtubules. The partition coefficient, which describes the probability of ATP synthesis, is equal to the rate of ATP synthesis divided by the sum of the rate of ATP synthesis plus the rate of phosphate release, $P_c = k_{-2}/(k_{-2} + k_3)$, with rate constants defined according to Scheme I. It is unlikely that the rates of ATP synthesis and phosphate release changed equally to maintain a constant partition coefficient. Therefore, we conclude that the rate of ATP synthesis, k_{-2}, and the rate of phosphate release, k_3, are not affected by microtubules, as they occur and contribute to the observed exchange reaction.

One must be careful not to take these conclusions out of context. The available data indicate that the dynein does not catalyze the exchange reaction while it is bound to a microtubule and, accordingly, the microtubules must inhibit the synthesis of ATP at the active site. The partition coefficient is a function of the change in the distribution of observed phosphate species and therefore depends only upon those reactions that do occur. The apparent inconsistencies between the conclusion that microtubules inhibit ATP synthesis and the failure to see any effect of microtubules on the partition

coefficient can be easily reconciled: Only free dynein catalyzes the reversible synthesis of ATP as measured by the exchange reactions.

This was further explored by examining the effect of microtubules on the exchange reaction in the presence of ADP. Microtubules markedly inhibited the rate of exchange at concentrations of ADP sufficient to saturate the rate of exchange catalyzed by free dynein (Figure 2). Increasing concentrations of ADP led to increasing rates of exchange which paralleled the dissociation of dynein from the microtubule. The direct correlation argues that only free dynein catalyzes the exchange reaction, and therefore microtubules must inhibit either phosphate binding or ATP synthesis or both.

The ADP concentration dependence of M·D dissociation and the rate of oxygen exchange could be fit to an equation based upon three independent and identical ATPase sites. According to this model, all three heads must bind ADP before the dynein can dissociate from the microtubule. The apparent K_d = 10–13 mM for ADP binding to the M·D complex is much larger than the value estimated from the inhibition of ATP-induced dissociation (0.4 mM). To a certain extent, the weaker binding of ADP to the M·D complex reflects the change in free energy associated with the power stroke in the rebinding of dynein to the microtubule. However, ADP alone does not cause the dynein to dissociate from the microtubule, and the apparent K_d observed for the dissociation and exchange reactions must be a function of the phosphate concentration and the free energy of formation of the M·D complex. Therefore, the value of 10–13 mM is probably an underestimate of the K_d for the M·D·ADP $\rightleftarrows$ M·D + ADP equilibrium.

ADP inhibited the rate at which ATP induced the dissociation of the microtubule–dynein complex. Analysis of the ATP and ADP concentration dependence of this reaction led to two important conclusions. The analysis of the competitive binding of ADP at the ATPase sites provided an estimate of the true K_d = 0.4 mM. Moreover, the kinetics demonstrated that the rate of release of ADP from the M·D·ADP complex was quite fast ($k_4' \simeq 1000\ s^{-1}$). Recent studies on the activation of the ATPase by cross-linking dynein to microtubules provided another estimate of the maximum rate of ATP turnover of 150 s^{-1} (Shimizu and Johnson, unpublished results). Considering the potential for systematic errors in either of these estimates, it is possible that each provides a measurement of the same rate-limiting step that would control the maximum rate of force production during the crossbridge cycle However, it is also likely that the two experiments are a function of different steps in the reaction sequence. Analysis of the ATPase pathway with the free dynein suggested that there must be two D·ADP states; one high-energy state is formed only upon phosphate release during ATP turnover and is distinct from the state formed by binding ADP from solution as shown in Scheme II. Accordingly microtubules bind to the high-energy D·ADP* state and induce a conformational change at a rate of 150 s^{-1}, perhaps accompanying crossbridge movement, which is then followed by a more rapid dissociation of ADP from an M·D·ADP state.

Scheme II

$$D + ATP \rightleftarrows D{\cdot}ATP \rightleftarrows D{\cdot}ADP{\cdot}P_i \rightleftarrows D{\cdot}ADP^* \rightleftarrows D{\cdot}ADP \rightleftarrows D + ADP$$

This model also provides a quantitative explanation for the thermodynamic parameters governing ADP binding. The K_d for ADP binding to the microtubule–dynein complex (0.37 mM) is comparable to the dissociation constant for the dynein–ADP complex (0.085 mM). The additional step from D·ADP* → D·ADP provides the free energy change available to do work associated with ADP release.

Support for this hypothesis comes from the microtubule binding experiments. The rates of binding of dynein to microtubules were 1.6×10^6 and $9.8 \times 10^5\ M^{-1}\ s^{-1}$ in the absence and presence of ADP, respectively. Omoto and Johnson (1986) measured a second-order rate constant for the binding of the dynein–products complex to the microtubule of $1.2 \times 10^4\ M^{-1}\ s^{-1}$. Accordingly, it would appear that the rate of binding of the D·ADP complex is 100-fold faster than the rate of binding to the D·ADP* complex, formed during ATP turnover. Although there is no direct evidence for the D·ADP* state, thermodynamic and kinetic arguments necessitate that there be an additional step (Holzbaur & Johnson, 1988).

An analysis of the thermodynamics of the microtubule–dynein ATPase cycle provides insight into the mechanism of energy transduction in this system. The data are consistent with a model based on the general principles of free energy transduction in biological systems described by Eisenberg and Hill (1985) and by Jencks (1980). In the crossbridge cycle, ATP binding drives the dissociation of the dynein heads. A large free energy change for ATP binding is required to overcome the tight binding of the microtubule–dynein complex. The overall ΔG for the reaction of M·D + ATP $\rightleftarrows$ M + D·ATP is small because it represents a small difference between two large values. ATP hydrolysis occurs near equilibrium at the active site of free dynein. However, in contrast to myosin, phosphate release is rapid, leading to formation of a high-energy D·ADP* state. These reactions conserve the free energy of nucleotide binding in the form of an activated state with ADP tightly bound. The D·ADP* complex then rebinds to the microtubule, and the stored free energy is lost upon ADP release and the re-formation of the microtubule–dynein complex. In vitro, the energy is dissipated to the solution, but in vivo, the free energy is coupled to the sliding of adjacent microtubules in the axoneme.

References

Barshop, B. A., Wrenn, R. F., & Frieden, C. (1983) *Anal. Biochem. 130*, 134–145.

Carlier, M. F., & Pantaloni, D. (1983) *Biochemistry 22*, 4814–4822.

Domanico, P. L., Rahil, J. F., & Benkovic, S. J. (1985) *Biochemistry 24*, 1623–1628.

Eisenberg, E., & Hill, T. L. (1985) *Science (Washington, D.C.) 227*, 999–1006.

Fairbanks, G., Steck, T. L., & Wallach, D. F. H. (1971) *Biochemistry 10*, 2606–2617.

Gibbons, I. R. (1981) *J. Cell Biol. 91*, 107s–124s.

Hackney, D. D. (1980) *J. Biol. Chem. 255*, 5320–5328.

Hackney, D. D. (1988) *Proc. Natl. Acad. Sci. U.S.A. 85*, 6314–6318.

Hackney, D. D., & Clark, P. K. (1984) *Proc. Natl. Acad. Sci. U.S.A. 81*, 5345–5349.

Hackney, D. D., Stempel, K. E., & Boyer, P. D. (1980) *Methods Enzymol. 64*, 60–83.

Holzbaur, E. L. F., & Johnson, K. A. (1986) *Biochemistry 25*, 428–434.

Holzbaur, E. L. F., & Johnson, K. A. (1989) *Biochemistry 28*, 5577–5585.

Holzbaur, E. L. F., Marchese-Ragona, S. P., & Johnson, K. A. (1986) *Biophys. J. 49*, 77a.

Jencks, W. P. (1980) *Adv. Enzymol. Relat. Areas Mol. Biol. 51*, 75–106.

Johnson, K. A. (1983) *J. Biol. Chem. 258*, 13825–13832.

Johnson, K. A. (1985) *Annu. Rev. Biophys. Biophys. Chem. 14*, 161–188.

Krauhs, E., Little, M., Kempf, T., Hofer-Warbinek, R., Ade, W., & Ponstingl, H. (1981) *Proc. Natl. Acad. Sci. U.S.A. 78*, 4156–4160.
Laemmli, U. K. (1970) *Nature (London) 227*, 680–685.
Lanzetta, P. A., Alvarez, L. J., Reinach, P. S., & Candia, O. A. (1979) *Anal. Biochem. 100*, 95–97.
Lymn, R. W., & Taylor, E. W. (1971) *Biochemistry 10*, 4617–4624.
Omoto, C. K., & Johnson, K. A. (1986) *Biochemistry 25*, 419–427.
Ponstingl, H., Krauhs, E., Little, M., & Kempf, T. (1981) *Proc. Natl. Acad. Sci. U.S.A. 78*, 2757–2761.
Porter, M. E., & Johnson, K. A. (1983a) *J. Biol. Chem. 258*, 6575–6581.
Porter, M. E., & Johnson, K. A. (1983b) *J. Biol. Chem. 258*, 6582–6587.
Schiff, P. B., Frant, J., & Horwitz, S. B. (1979) *Nature (London) 277*, 665–667.
Shimizu, T., & Johnson, K. A. (1983) *J. Biol. Chem. 258*, 13841–13848.
Taylor, E. W. (1979) *CRC Crit. Rev. Biochem. 6*, 103–164.

Activation of the Dynein Adenosinetriphosphatase by Cross-Linking to Microtubules†

Takashi Shimizu,‡ Silvio P. Marchese-Ragona, and Kenneth A. Johnson*
Department of Molecular and Cell Biology, The Pennsylvania State University, University Park, Pennsylvania 16802
Received November 29, 1988; Revised Manuscript Received April 26, 1989

ABSTRACT: The microtubule–dynein complex consisting of 22S dynein from *Tetrahymena* cilia and MAP-free microtubules was subjected to treatment with various concentrations of 1-ethyl-3-[3-(dimethylamino)-propyl]carbodiimide (EDC), a zero-length cross-linker, at 28 °C for 1 h. Following cross-linking of the microtubule–dynein complex, nearly all of the ATPase activity cosedimented with the microtubules in the presence of ATP. Electron microscopic observation by negative staining revealed that, following treatment with 1 mM EDC, the complex did not dissociate in the presence of ATP, although the dynein decoration pattern was disordered. The complex treated with 3 mM EDC exhibited normal microtubule–dynein patterns even after the addition of ATP. The ATPase activity of the microtubule–dynein complex was enhanced about 30-fold by the treatment with 1–3 mM EDC. These results indicate that the ATPase activation was caused by the close proximity of the dynein ATPase sites to the microtubules and provide further support for the functional interaction of all three dynein heads with the microtubule. The maximal specific activity was 12 μmol min^{-1} (mg of dynein)$^{-1}$, corresponding to a turnover rate of 150 s^{-1}, which may be the rate-limiting step at infinite microtubule concentration and may represent the maximum rate of force production in the axoneme.

Axonemal dynein from cilia or flagella couples the hydrolysis of ATP to produce a force for microtubule sliding [for reviews, see Gibbons (1981) and Johnson (1985)]. Recent work has demonstrated a related cytoplasmic dynein in numerous cell types (Hisanaga & Sakai, 1983; Asai & Wilson, 1985; Paschal & Vallee, 1987; Pratt, 1986). Depending on the source of its isolation, dynein is composed of 2 or 3 polypeptides with a molecular weight of 400 000 or more (Mabuchi & Shimizu, 1974; Bell, 1983; Lee-Eiford et al., 1986), 2 or 3 intermediate chains, and 8–10 low molecular weight chains. *Tetrahymena* dynein, used in this study, has three globular heads connected to a common base by three strands and a net molecular weight of 1.9 million (Johnson & Wall, 1983). This dynein adenosine-5′-triphosphatase (ATPase)[1] has been shown to have an ATPase mechanism similar to that of actomyosin (Johnson, 1985) and serves as the paradigm for understanding the ATPase mechanism of all dyneins.

One of the characteristics of dynein is its ATP-sensitive binding to microtubules (Haimo et al., 1979; Porter & Johnson, 1983a,b; Omoto & Johnson, 1986). This microtubule–dynein complex constitutes a simple model system for cilia or flagella, as actomyosin is for muscle. Omoto and Johnson (1986) have demonstrated activation of the dynein ATPase by a high concentration of the microtubules free from microtubule-associated proteins (MAPs) under physiological conditions. Their study indicated that activation of the dynein ATPase required a high concentration of the MAP-free microtubules which could be rationalized in terms of the very high local concentration of microtubules in the axoneme. ATPase activation was also observed at low microtubule concentrations if the ATP concentration was sufficiently low to allow the dynein to remain transiently tethered to the microtubule by one of the three heads. For the current work, we reasoned that if dynein could be cross-linked to the mi-

† This work was supported by NIH Grants GM26726 and GM32023 to K.A.J. K.A.J. was supported by an Established Investigatorship from the American Heart Association with funds contributed in part by the Pennsylvania Affiliate.
* Author to whom correspondence should be addressed.
‡ Present address: Research Institute for Polymers and Textiles, Higashi, Tsukuba, Ibaraki 305, Japan.

[1] Abbreviations: ATPase, adenosine-5′-triphosphatase; EDC, 1-ethyl-3-[3-(dimethylamino)propyl]carbodiimide; HEPES, *N*-(2-hydroxyethyl)piperazine-*N*′-2-ethanesulfonic acid; MAP(s), microtubule-associated protein(s); PIPES, 1,4-piperazinediethanesulfonic acid; SDS, sodium dodecyl sulfate.

0006-2960/89/0428-7016$01.50/0